

On Counter-Charges in Development Rollers for Electrophotography

Inan Chen and Ming-Kai Tse; Quality Engineering Associates (QEA), Inc.; Burlington, MA, USA

Abstract

The roles of counter-charges in toner charging and toner deposition processes for single-component development are studied by quantitative analyses of charge injection into and transport through the development rollers, taking into consideration the non-Ohmic nature of the semi-insulating overcoat layer of the rollers. The electrical requirements for the roller coatings, especially as a consequence of increased printing speed, are elucidated. Based on the findings, an ideal evaluation technique for development roller performance is suggested.

Introduction

In electrophotography, latent images are developed by moving charged toners from their suppliers to the photoreceptors. Extensive works on the measurements and analyses of toner motion have been reported in the literature.¹⁻⁴ In contrast, little attention has been paid to the motion of counter-charges that reside on the toner suppliers, namely, the carrier beads that form magnetic brushes in two-component development, or the development rollers in single-component development (SCD). In the development process, toners are electrostatically attracted not only to the charges of latent images but also to the counter-charges in the opposite direction. Toner motion toward the latent images can be seriously impeded if the counter-charges are not efficiently neutralized, especially as the print speed increases and the development time is shortened.

Experimental observations suggest that in SCD, toners are predominantly charged during their contact with the metering blade. At the same time, counter-charges are induced in the roller. Thus, the amount of charge that toners can acquire in a given charging time is controlled by the efficiency of counter-charge induction.

In this paper, we investigate the roles of counter-charges on toner charging and deposition in SCD by quantitative analyses of charge injection and transport in the thin (about 10^{-2} cm) semi-insulating (i.e. highly resistive) overcoat layer of the development rollers. Similar charge transport analyses have recently been applied to electrostatic transfer of developed images,⁵ and roller charging of photoreceptors.⁶ The analysis is based on a first principle charge transport theory, taking into consideration the non-Ohmic nature of charge injection in the overcoat layer. The charging step is considered first (next section). The toner deposition step is analyzed subsequently. Based on the findings of this study, an ideal evaluation method for development roller performance is suggested.

Toner Charging Process

Figure 1 shows a layer model of toner charging at the metering blade. The blade is sufficiently conductive in practice. A

bias voltage V_b is applied across the toner and the roller coating (RC) layers. Denoting the layer thickness by L_k , the permittivity by ϵ_k and defining $D_k = L_k/\epsilon_k$, with the subscript $k = t$ and r referring to toner and RC layers, respectively, the fields $E_k(y)$ and voltages V_k across layer k , at a given time, can be expressed as follows.

In the toner layer:

$$E_t(y) = (q_t/\epsilon_t)y_t \quad (1)$$

$$V_t = -(q_t/\epsilon_t)L_t^2/2 = -Q_t D_t/2 \quad (2)$$

where q_t is the volume charge density in the toner layer, assumed to be uniform across the toner layer, and is a function of charging time.

In the RC layer:

$$E_r(y_r) = E_{r0} + \int_0^{y_r} [q_p(y') + q_n(y')] dy'/\epsilon_r \quad (3)$$

$$V_r = -(E_{r0}L_r + U_r) = -(Q_t + Q_r)D_r - U_r \quad (4)$$

where E_{r0} is the field at the toner/RC interface, and

$$U_r = \int_0^{L_r} dy' \int_0^{y'} [q_p(y') + q_n(y')] dy'/\epsilon_r \quad (5)$$

is the integral of positive and negative charge densities, $q_p(y,t)$ and $q_n(y,t)$ in the semi-insulating RC layer. In Eq.(4), E_{r0} is expressed in terms of toner layer total charge $Q_t = q_t L_t$ and the charge at the interface Q_r using Gauss' theorem. Equating the sum of V_t and V_r to $-V_b$ (≤ 0) the toner charge q_t can be expressed as,

$$q_t = Q_t/L_t = (V_b - U_r - Q_r D_r)/(D_t/2 + D_r)L_t \quad (6)$$

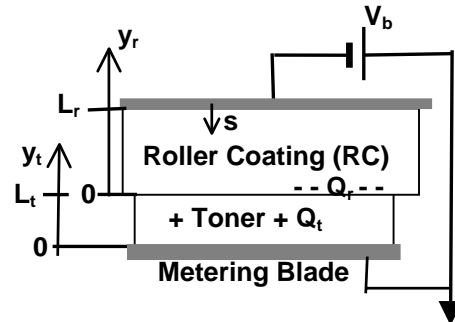


Fig. 1 Layer model of SCD toner charging at metering blade.

Assuming (without loss of generality) that the toners are charged positive ($q_t > 0$), then, negative counter-charges are induced in the RC layer, e.g. by injection of negative charges from the bias and/or removal of positive charges from the RC layer. This makes U_r and Q_r more negative and hence, q_t more positive (Eq. 6).

The charge densities in RC, q_p and q_n , vary with time t from the initial (intrinsic) value $\pm q_i$, according to the continuity equations,

$$\partial q_p(y, t)/\partial t = -\partial J_p/\partial y, \quad \partial q_n(y, t)/\partial t = -\partial J_n/\partial y, \quad (7)$$

with, $J_p(y, t) = \mu_p q_p E_r$, $J_n(y, t) = \mu_n q_n E_r$ (8) where J_p (or J_n) and μ_p (or μ_n) are the positive (or negative) conduction current and charge mobility, respectively. The (negative) current injected from the bias is assumed to be proportional to the field $E_r(L_r)$ at the RC-to-bias contact, $y = L_r$,

$$J_n(L_r) = s E_r(L_r) \quad (9)$$

where s is a parameter specifying the injection strength. All the fields E are related to the charge densities by Poisson's equation.

The results of numerical calculations are presented in normalized units listed in Table I. The first four basic units are used to define the next five derived ones. The typical values of the units for practical interest in this discussion are also given in the table.

Table I. Normalized Units

| Units | Typical Values |
|---|---|
| Length: L_o | 10^{-2} cm |
| Permittivity: ϵ_o | 3×10^{-13} F/cm |
| Voltage: V_o | 10^3 V |
| Charge mobility: μ_o | 10^{-5} cm ² /Vsec |
| ----- | |
| Field: $E_o = V_o/L_o$ | 10^5 V/cm |
| Time: $t_o = L_o/\mu_o E_o = L_o^2/\mu_o V_o$ | 10^{-2} sec |
| Charge density /area: $Q_o = \epsilon_o E_o$ | 3×10^{-8} Coul/cm ² |
| Charge density /vol.: $q_o = Q_o/L_o$ | 3×10^{-6} Coul/cm ³ |
| Injection strength and Conductivity: $\sigma_o = \mu_o q_o$ | 3×10^{-11} S/cm |

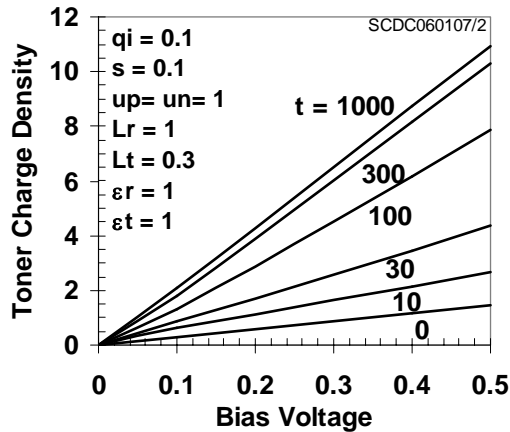


Fig. 2. Time and bias voltage dependence of toner charge density q_t (in normalized units of Table I)

Figure 2 shows the increase of toner charge density q_t with bias voltage V_b and charging time t , calculated with the parameter values shown in the figure. The dependence of q_t on V_b is quite linear at a given time. The increase of q_t with time saturates to an asymptotic value that depends on V_b .

The growth of toner charge with time is illustrated in more details in Figs. 3 and 4. The dependence on the injection strength s of the counter-charge is shown in Fig.3. Other parameter values common to all curves are given in the figure. It can be seen that with smaller s , it requires longer time for the toner charge to reach the asymptotic value. Thus, as the charging time becomes shorter (e.g., due to increased print speed) it is more important to have a good injection of counter-charges from the bias electrode.

Figure 4 shows the dependence on charge mobilities, μ_p and μ_n . For positive toner charge (i.e., negative counter-charge), the size of μ_n has significant effect on the charging rate (compare curves A, B, C), while the reduced μ_p value has no unfavorable effect (compare curves A and D). This indicates that the major contribution to the counter-charges comes from negative charge injection from the bias, and not from the depletion of positive charges in the RC layer. Calculations with other parameter values within the range of practical interest have produced the same feature:

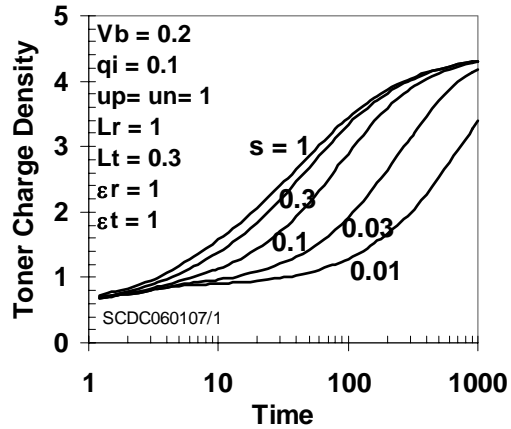


Fig. 3. Time evolution of toner charge q_t for various injection strength s (in normalized units of Table I)

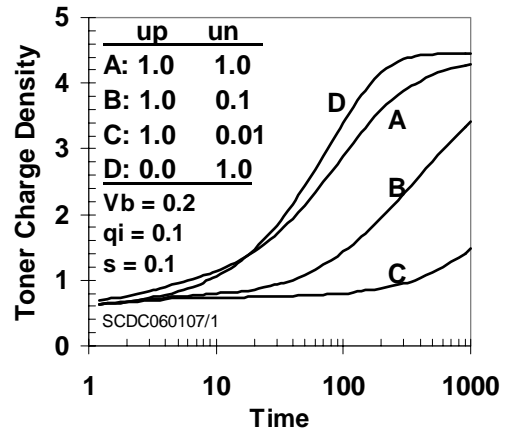


Fig. 4. Charge mobility dependence of the growth of toner charge q_t (in normalized units of Table I)

Toner Deposition Process

The configuration at the development nip is represented by a one-dimensional three-layer system consisting of the semi-insulating roller-coating layer (RC), the toner layer and the grounded photoreceptor (PR), as shown in Fig. 5. A small air gap that may exist (e.g., in non-contact SCD) between the toner layer and the PR makes no physically significant difference in this discussion.

The PR is assumed to be space charge free, with a uniform field E_p across the layer and hence, the voltage over the layer is $V_p = -E_p L_p$. The toner layer is assumed to have a constant and uniform volume charge density q_t , thus, the field and the voltage are,

$$E_t(y_t) = E_{t0} + (q_t/\epsilon_t)y_t \quad (10)$$

$$V_t = -(E_{t0} + q_t L_t/2\epsilon_t)L_t = -(E_{t0} + Q_t/2\epsilon_t)L_t \quad (11)$$

where E_{t0} is the toner layer field at the toner/PR interface.

In the RC layer, the field $E_r(y)$ and the voltage V_r are expressed in terms of the field E_{r0} at the RC/toner interface, the densities $q_p(y)$ and $q_n(y)$ of positive and negative mobile charges as,

$$E_r(y_r) = E_{r0} + \int_0^{y_r} [q_p(y') + q_n(y')] dy' / \epsilon_r \quad (12)$$

$$V_r = -\int_0^{L_r} E_r(y) dy = -(E_{r0} L_r + U_r) \quad (13)$$

with U_r given by Eq.(5).

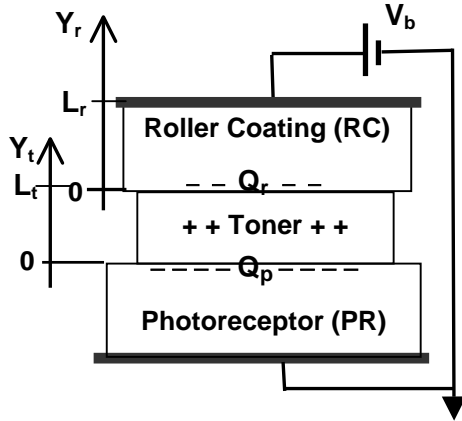


Fig. 5 Layer model of development nip in SCD

Denoting the PR surface charge density by Q_p , and the charge at toner/RC interface by Q_r , Gauss' theorem can be used to relate the fields E_p and E_{r0} to E_{t0} as follows:

$$E_p = (\epsilon_t E_{t0} - Q_p) / \epsilon_p \quad (14)$$

$$E_{r0} = (\epsilon_t E_{t0} + Q_r + Q_t) / \epsilon_r \quad (15)$$

Then, equating the sum of voltages V_p , V_t and V_r to the bias voltage V_b , one obtains the fields E_{t0} as,

$$E_{t0} = [V_d - Q_t(D_r + D_t/2) - Q_r D_r - U_r] / \epsilon_t (D_p + D_t + D_r) \quad (16)$$

where $V_d = Q_p D_p - V_b$, is the development voltage, and $D_r = L_r / \epsilon_r$, $D_t = L_t / \epsilon_t$, $D_p = L_p / \epsilon_p$.

For positively charged toners ($Q_t > 0$), negative E_t is required for toner deposition on PR. A demarcation line that separates the

toner layer with $E_t(y_t) < 0$ from that with $E_t(y_t) > 0$ can lie within the toner layer at $y_t = Y_d$, with $E_t(Y_d) = 0$. The ratio of Y_d to the toner layer thickness L_t can be used to represent the extent or the "efficiency" of toner deposition. Then, using Eqs.(10) and (16), the deposition efficiency Y_d/L_t is given by,

$$Y_d/L_t = -\epsilon_t E_{t0} / q_t L_t = -\epsilon_t E_{t0} / Q_t = -[V_d - Q_t(D_r + D_t/2) - Q_r D_r - U_r] / Q_t (D_p + D_t + D_r) \quad (17)$$

Based on the results of the previous section (on charging), between the end of charging and the beginning of deposition, most of the counter-charges are located at the RC/toner interface and the RC layer is nearly in equilibrium. Thus, starting with the initial condition that: $Q_r \approx -Q_t$, and $U_r \approx 0$ at $t = 0$, the demarcation line Y_d shifts upward with time as the counter-charges are neutralized by injection of positive charges from the bias or removal of negative charges in the RC bulk.

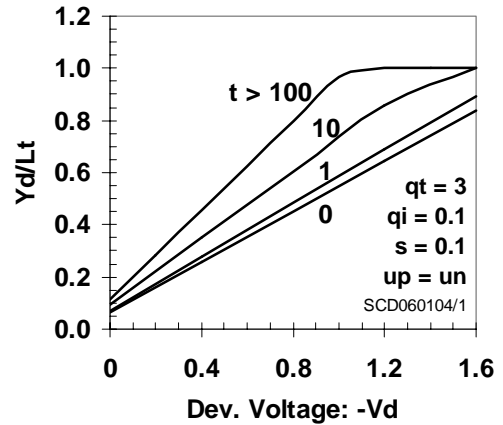


Figure 6. Dependence of deposition efficiency, Y_d/L_t on (negative of) development voltage and time (in normalized units of Table I)

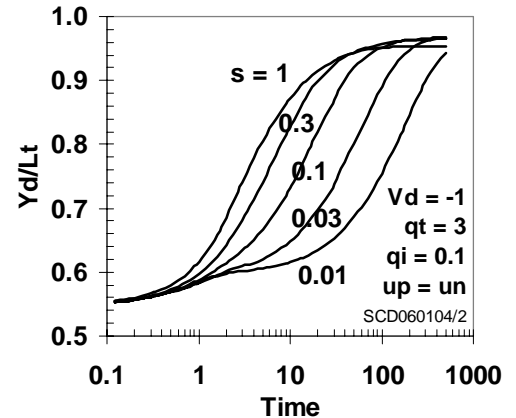


Figure 7. Growth of deposition efficiency Y_d/L_t with time, as injection strength s is varied (in normalized units of Table I)

The transport of charges in RC is governed by the continuity equations as described in the previous section on charging, Eqs. (7, 8, 9). These equations are used to calculate U_r and Q_r as functions of time, and used in Eq. (17) for the deposition efficiency $Y_d(t)/L_t$.

Numerical results presented and discussed in the following figures are calculated with the thickness: $L_r = 1$, $L_t = 0.3$, $L_p = 0.25$, and the permittivity: $\epsilon_r = 1$, $\epsilon_t = 1$, $\epsilon_p = 0.25$. But, the conclusions are not affected by these parameter values within the range of practical interest.

The deposition efficiency Y_d/L_t increases with the (negative of) development voltage V_d and time as shown in Fig. 6. It reaches the maximum value of unity at large $|V_d|$ or long time, as expected. Figure 7 shows the time evolution of the deposition efficiency for five values of s , the strength of charge injection from the bias, with a set of (typical) V_d , q_t , and q_i values given on the figure. In these curves, the mobilities of positive and negative charges are assumed to be equal. It can be seen that although the asymptotic value of deposition efficiency is independent of s , the time it takes to reach the latter value increases by an order of magnitude as s decreases by one to two orders of magnitude. The injected charges contribute to the neutralization of the (pre-existing) counter-charges (Q_r). Consequently, a difference in toner deposition can result from the difference in the injection strength of charge if the development time is less than a few 100's time units t_0 (typically $t_0 \approx 10^{-2}$ sec, Table I).

The effects of charge mobilities, μ_p and μ_n , on the growth of deposition efficiency Y_d/L_t are shown in Fig. 8. Curve-A shows the growth of Y_d/L_t with time for a sample with $q_i = 0.1$, $s = 0.1$ and equally mobile positive and negative charges, $\mu_p = \mu_n = 1$. In curves B and C, the positive charge mobility is reduced to $\mu_p = 0.1$ (B) and $\mu_p = 0.01$ (C), respectively. This slows down the contribution of injected positive charges in the neutralization of counter-charges, and hence, the growth of the deposition efficiency. In contrast, when the negative charge mobility is reduced, as in curve D ($\mu_n = 0.01$) the growth of deposition efficiency is hardly affected.

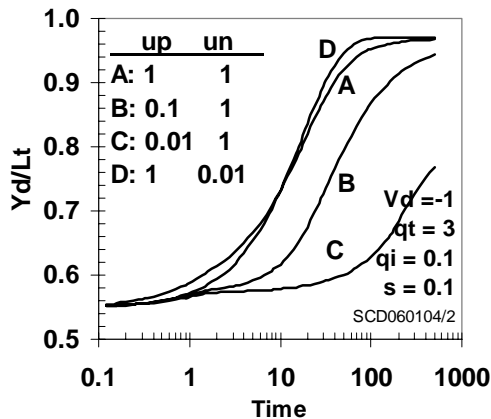


Figure 8. Effects of charge mobility on deposition efficiency Y_d/L_t (in normalized units of Table I)

Conclusions

The above analyses have shown that in SCD, the induction and neutralization of counter-charges in development rollers play important roles in toner charging and deposition, respectively. By considering the non-Ohmic nature of charge injection in the semi-insulating roller-coating layer, the analyses further indicate that

efficient charge injection from the bias electrode and transport in the layer are required to complete the charging and deposition processes in a time of the order of one hundred time units t_0 . With ever increasing print speeds, for the available process time to satisfy this requirement, the time unit t_0 should be small. The time unit, $t_0 = L_r^2/\mu_0 V_d$, is defined (in Table I) in terms of roller-coating layer thickness L_r , development voltage V_d and charge mobility μ_0 . Therefore, it can be shortened with high charge mobility in the overcoat layer. Unfortunately, there is little information on the mobility values in the coating materials.

Furthermore, the results from the above two sections show that for positive toners, in addition to a sufficient injection strength (with $s > 0.1$), a good negative charge mobility is required for toner charging (Fig. 4), while a good positive charge mobility is required for toner deposition (Fig. 8). This means that an ideal roller-coating layer should be ambi-polar in charge transport. Unfortunately, the roller-coating layers are usually made of polymeric materials, which often exhibit much different mobilities for positive and negative charges.

Traditionally, the performance of development rollers is evaluated by measuring the electrical resistance. However, it has been known that the roller resistance, determined from closed-circuit constant-voltage measurements, can fluctuate from measurements to measurements, depending on the contact conditions, and are often inconsistent with the device performance. Furthermore, resistance values do not specify the polarities of mobile charges or confirm the ambi-polarity of charge transport. We have introduced an alternative technique, known as "Electrostatic Charge Decay (ECD)",⁸⁻¹⁰ that carries out automated and non-destructive (non-contact) electrical characterizations of semi-insulating roller-coating layers (and other semi-insulator devices for electrophotography). The technique is based on the measurements of open-circuit voltage decay during and/or after corona charging of the roller-coating surface. Since the measurement technique closely simulates the actual dielectric relaxation process in electrophotography, the results are expected to be more useful in predicting electrophotographic performance.

References

- [1] J. Shaw and T. Retzlaff, Proc. IS&T's NIP-12, pg.283 (1996)
- [2] H. Mizes, J. Beachner, P. Ramesh, and K. German, Proc. IS&T's NIP-14, pg.409 (1998)
- [3] J. Hirabayashi, Proc. IS&T's NIP-19, pg.18 (2003)
- [4] J. Yi, Proc. IS&T's NIP-21, pg.586 (2005)
- [5] I. Chen, Proc. IS&T's NIP-20, pg. 30 (2004)
- [6] I. Chen and M.-K. Tse, Proc. IS&T's NIP-21, pg. 566 (2005)
- [7] I. Chen and M.-K. Tse, J. Imag. Sci. & Tech. **44**, 462 (2000)
- [8] M.-K. Tse, D. Forest and F. Y. Wong, Proc. IS&T's NIP-11, pg. 383 (1995)
- [9] I. Chen and M.-K. Tse, Proc. IS&T's NIP-17, pg. 92 (2001)
- [10] M.-K. Tse and I. Chen, Proc. Japan Hardcopy-2005, pg. 199 (2005)

Author Biography

Inan Chen received his Ph.D. from the University of Michigan in 1964, and worked at Xerox Research Laboratories in Webster, NY, from 1965 to 1998. Currently, he is a consulting scientist for Quality Engineering Associates (QEA), Inc. and others. He specializes in mathematical analyses of physical processes, in particular, those related to electrophotographic technologies. He is the recipient of IS&T's 2005

Chester F. Carlson Award. Contact at inanchen@frontiernet.net or www.qea.com